Eng. & Tech. Journal ,Vol. 27, No. 14,2009

Numerical Study Of Turbulent Natural Convection In An Enclosure With Localized Heating From Left Side

Ali L. Ekaid

Received on:24/11/2008
Accepted on:7/5/2009

Abstract

In this work, a numerical study is performed to predict the solution of buoyancy turbulent flow and heat transfer inside a square cavity with localized heating from the left side wall. Full Navier Stockes and energy equations were solved using Finite volume method with a non-uniform staggered grid. The studied Rayleigh numbers were ranged between $1E10^{8}$ to $1E10^{12}$ and Pr=0.72. For the purpose of the analysis, the heated dimensionless length L/H is varied from 0.2 to 0.8. The k-ε model with standard wall function is used to treat the turbulence in the flow. The obtained results show that the strength of the induced recirculating velocity is increased with the increase of Ra. Also the results displaced that the average Nu is increased with the increase of Ra. However the average Nu number is decreased with increasing of dimensionless heated length.

Keywords: Natural convection; Turbulent; CFD.

دراسة عددية لانتقال الحرارة الحر المضطرب داخل فجوة بوجود عنصر تسخين على الجدار الايسر

الخلاصة

في هذا البحث أجريت دراسة عددية لتخمين انتقال الحرارة بالحمل الحر الاضطرابي وكذلك جريان المائع داخل حيز مربع الشكل مع وجود تسخين موضعي للجدار الايسر من الحيز. تم حل معادلات نافيرو ستوك ومعادلة الطاقة بأستخدام طريقة الحجم المحدد وبأستخدام نظام الشبكة الزاحفة الغير منتظمة. تراوحت أعداد رايلي المدروسة في هذا البحث بين $1E10^{8}$ و $1E10^{12}$ ،بينما عدد برانتدل كان ٠.٧٢ والمسافة اللابعدية لمصدر التسخين L/H تتراوح بين ٠.٢ الى ٠.٨ . نموذج k-ε الاضطرابي ودالة الجدار تم استخدامها لمعالجة الاضطراب في الجريان. بينت النتائج التي تم الحصول عليها ان شدة الدوامات الدوارة تزادت مع زيادة عدد رايلي. كذلك بينت النتائج ان متوسط نسلت يزداد مع زيادة عدد رايلي ويقل مع زيادة طول الجزء المسخن من جدار الحيز.

Introduction

Natural convection heat transfer in enclosures is found in multiple engineering fields such as solar collectors, electronic equipment cooling and energy transfer in buildings and nuclear reactors.

Also the natural convection in these enclosures or cavities was a good tool for the computational and experimental studies. Because the complex phenomena inherent in the structure and behavior of the fluid flow and heat transfer in these enclosures, the additional research is needed.

References [1] to [8] reviewed multiple numerical and experimental studies on the laminar and turbulent heat transfer in the enclosures. The problems found in these studies are the boundary conditions and the stability of the numerical solutions at high Rayleigh numbers. The grid points and a computational time was a function of Rayleigh number. In other side, in nuclear power plants compartments, sometime happens ,a combustion from the leak of combustible liquid material from pipe lines. The heat of combustion is transferred through the compartments

* Machine and Equipment Engineering Department, University of Technology / Baghdad

https://doi.org/10.30684/etj.27.14.14
2412-0758/University of Technology-Iraq, Baghdad, Iraq

by a natural convection. Aydin and Yang [9]used a computational study on laminar natural convection in a rectangular enclosure with localized heating from below. They studied the effect of the size of the heat source and Ra on the flow field and heat transfer characteristics. Calcagni at al. [10] studied the natural convection heat transfer numerically and experimentally in square enclosure heated from below. The study was focused on the calculation of local and average Nusselt number on the heat source. The current study as shown in Figure(1) is focused on the natural convection heat transfer in a square enclosure heated from left side.

Problem description

The problem studied in this paper is a two dimensional turbulent buoyancy flow and heat transfer in a square cavity with localized heating from left side. The two vertical walls having an isothermal temperature except the heat source which has a higher a temperature, The upper and lower walls are insulated. The considered Rayleigh numbers was ranged from (10^8) to (10^{12}), The working fluid was air with Pr=0.72 .The heat source position and the size is changed for different values on the left hand side The changing of the location of heat source to the left side wall instead of a bottom wall has a great effect on the structure of the flow and heat transfer besides to the Nu. From the familiar facts that if the localized heating from the below, the physical explanation of the thermal and flow field is known but there is unknown expected phenomena when the localized heating is not from below. Figure(2) shows the physical problem.

Mathematical model

The two dimensional buoyancy driven turbulent flow and heat transfer in a square cavity are described by the steady Navier-Stokes and energy equations. The density of air is assumed constant except in the gravity force which is assumed to be linearly dependence on the temperature introduced. Therefore these equations are expressed as follows [11] :

$$\frac{\partial}{\partial x}(r u)+\frac{\partial}{\partial y}(r v)=0 \qquad \ldots(1)$$

$$\frac{\partial}{\partial x}(r uu)+\frac{\partial}{\partial y}(r vu)=-\frac{\partial p}{\partial x}+\frac{\partial}{\partial x}\left[2m_{eff}\frac{\partial u}{\partial x}\right]+\frac{\partial}{\partial y}\left[m_{eff}\left(\frac{\partial u}{\partial y}+\frac{\partial v}{\partial x}\right)\right] \qquad \ldots(2)$$

$$\frac{\partial}{\partial x}(r uv)+\frac{\partial}{\partial y}(r vv)=-\frac{\partial p}{\partial y}+\frac{\partial}{\partial x}\left[m_{eff}\left(\frac{\partial v}{\partial x}+\frac{\partial u}{\partial y}\right)\right]+\frac{\partial}{\partial y}\left[2m_{eff}\frac{\partial v}{\partial y}\right]+r b g(T-T_o) \qquad \ldots(3)$$

$$\frac{\partial}{\partial x}(r uT)+\frac{\partial}{\partial y}(r vT)=\frac{\partial}{\partial x}\left[\Gamma_{eff}\frac{\partial T}{\partial x}\right]+\frac{\partial}{\partial y}\left[\Gamma_{eff}\frac{\partial T}{\partial y}\right] \qquad \ldots(4)$$

$$\Gamma_{eff}=\frac{m}{\Pr}+\frac{m_t}{\Pr_t} \qquad \ldots(5)$$

The equations of turbulence energy (k) and the dissipation rate (ε) proposed by Launder and Spalding [11], are described as follows;

$$\frac{\partial}{\partial x}(r uk)+\frac{\partial}{\partial y}(r vk)=\frac{\partial}{\partial x}\left[\left(m+\frac{m_t}{s_k}\right)\frac{\partial k}{\partial x}\right]+\frac{\partial}{\partial y}\left[\left(m+\frac{m_t}{s_k}\right)\frac{\partial k}{\partial y}\right]+G-re \qquad \ldots(6)$$

$$\frac{\partial}{\partial x}(r ue)+\frac{\partial}{\partial y}(r ve)=\frac{\partial}{\partial x}\left[\left(m+\frac{m_t}{s_e}\right)\frac{\partial e}{\partial x}\right]+\frac{\partial}{\partial y}\left[\left(m+\frac{m_t}{s_e}\right)\frac{\partial e}{\partial y}\right]+C_1\frac{e}{k}G-r C_2\frac{e^2}{k} \qquad \ldots(7)$$

Where

$$G=m_t\left[2\left(\frac{\partial u}{\partial x}\right)^2+2\left(\frac{\partial v}{\partial y}\right)^2+\left(\frac{\partial u}{\partial y}+\frac{\partial v}{\partial x}\right)^2\right] \qquad \ldots(8)$$

The turbulent viscosity is obtained by the following equation [11].

$$m_t=r C_u\frac{k^2}{e} \qquad \ldots(9)$$

For k-ε turbulent model, the constants used are C_u =0.09 ; C_1=1.44 ; C_2=1.92 ; σ_k=1.0 ; σ_ε =1.0.

The dimension stream function ψ is obtain by solving the following poisson equation with the boundary condition ψ=0 at all the solid wall.

$$\frac{\partial^2 y}{\partial x^2}+\frac{\partial^2 y}{\partial y^2}=\frac{\partial u}{\partial y}+\frac{\partial v}{\partial x} \qquad \ldots(10)$$

Boundary conditions

In order to solve the considered mathematical model, the following boundary condition are introduced:

- Top and bottom walls:

$\frac{\partial T}{\partial y}=0$,u = v = k =0 and $\frac{\partial e}{\partial y}=0$

- Right wall:

T = T_c ,u = v = k =0 and $\frac{\partial e}{\partial x}=0$

- Left wall:

T = T_c , for $0 \le x \le \left(\frac{1-L/H}{2}\right)H$ and $\left(\frac{1+L/H}{2}\right)H \le x \le H$

T = T_h , for $\left(\frac{1-L/H}{2}\right)H \le x \le \left(\frac{1+L/H}{2}\right)H$

u = v = k =0 and $\frac{\partial e}{\partial x}=0$

Nusselt number

The characteristic of the flow is the rate of heat transfer across the cavity. The Nusselt number on the heated dimensionless length (L/H) is calculated as :

$$Nu_y=\frac{\partial T}{\partial x}\frac{W}{(T_h-T_c)} \qquad \ldots(11)$$

$$\left.\frac{\partial T}{\partial x}\right|_{x=o}=\frac{q}{k} \qquad \ldots(12)$$

Where the heat flux at the wall, q is calculated from wall functions [12] . The heat transfer per unit area at the wall is then calculated from the following formula :

$q = St\ \rho|v|\ Cp\ (T_p - T_w)$ …(13)

Where;

$St = Cf * Pr^{-2/3}$ …(14)

$Cf = \tau_w /(\rho*|v|^2)$ …(15)

T_p is the temperature at grid node in question, and T_w is the temperature at the wall. The average Nusselt number is given by :

$$Nu=\int_{(\frac{1-L/H}{2})H}^{(\frac{1+L/H}{2})H}\left(\frac{\partial T}{\partial x}\right)dy\Big|_{x=0} \qquad \ldots(16)$$

Numerical method

The elliptic partial differential equations describing the flow field and heat transfer are discredited using finite volume method. This gives a system of algebraic equations. The solution of these equations is performed through a computer program. This program is developed to attain the numerical results of 2D buoyancy turbulent flows inside enclosure. The SIMPLE algorithm with implicit Gauss-elimination scheme are used [13]. Non uniform rectangular staggered grids in all directions are used.

These grids are finnier near the walls where gradients are important. One can mention here that the largest number of grid points lies in the boundary layers. The considered rectangular grids are staggered for vector variables and stored in the main positions for the scalar one. In order to accelerate the convergence in each iteration process, relaxation factors are incorporated. The relaxationion factors used for velocity components (u) (v), pressure (p) ,turbulence quantities

(k) (ε) and temperature are 0.4 , 0.4 , 0.5 , 0.7 , 0.7 , 0,7 respectively. The number of grid points is a function of Rayleigh number. For Ra ≤ 1E10, the grids number used is (61*61), Figure(3-a), and for Ra ≥ 1E10 the grid number used (81*81), Figure(3-b),

A converged solution was defined as one that meet the following criterion for all dependent variables. $\max\left|f^{n+1}-f^{n}\right|\leq 10^{-4}$.

Results and discussion

The results were obtained for Rayleigh number up to $1E10^{12}$. The heated dimensionless length L/H was ranged from 0.2 to 0.8. Hence the results are described as follows.

Figure (4) shows the distribution of stream function for different Rayleigh numbers and L/H=0.2, When $Ra=1E10^{8}$ there is three re-circulating vortices which have different sizes. As Rayleigh increases only two vortices are enlarged and the vortices lies in the left upper corner are become smaller. Also it can be seen that the values of stream function are increased with increase of Rayleigh number as shown in Figures (1),(2),(3),(4) and (5). Because when Ra increases, the buoyancy force is increased and leads to increase re-circulating vortices sizes. Also when Ra is increasing the location of these vortices is moved to upper side and that demonstrate the movement of circulating flow is concentrated in the upper part. Figure (5)shows the isothermal contours for the considered Rayleigh numbers and L/H=0.2 .The heat is transferred from the heat source through the working fluid to the remaining parts of the enclosure. The formation of the thermal boundary layer is obviously seen where the cold wall side temperature begins to rise and this increases with increase of Rayleigh number. As the dimension heated length is increased to 0.4 as shown in figure (6), the upper vorticity is some what be smaller. The strength of stream function becomes larger and this increases with increase of Ra. The temperature distribution for different Rayleigh numbers and L/H=0.4 is found in figure (7). It is clear that the temperature stratification is found in the enclosure core and thermal boundary layer on the cold and hot side is significantly effected with the increase of Ra. This behavior is dominant for the next cases at L/H=0.6 and L/H=0.8. The Stream function distribution is shown in figures (8) and (10) which show that re-circulating vorticities are changed to to one re-circulating vorticity and the location of this vorticity is moved to the upper of the enclosure and the strength of this vorticity is increased more with the increase of Ra as compared with other cases. The temperature distribution is effected with the increase of Ra as shown in figures (9) and (11). The thickness of the thermal boundary layer is decreased with the increase of Ra.

Figures (12) and (13) demonstrate the dimensionless horizontal and vertical components of the velocity computed at the domain center lines (using k/W as scale factor, where k is the thermal diffusivity). It is evident that the velocity maximum moves closer to the walls and its amplitude increases.

Figures (14) and (15) show the distribution of the average Nu versus Ra and dimensionless heated length respectively. It can be seen that the average Nusselt number increase with the increase of Ra for all the studied cases. However the values of Nu average decrease with the increase of the heated dimensionless length because when the heat source length increases, the temperature level of the left side wall

increases, leading to reduction in heat transfer coefficient which is inversely proportional to the wall temperature.

The present numerical results are compared with the published results as shown in Figure (16). From the figure, the comparison indicated a good agreement.

Conclusions

- The strength of the re-circulating vortices are increased with the increase of Ra. While the number of the resulted vortices are decreased.
- The Nusselt number is a strong function for a Rayleigh number and the dimensionless heated length.
- The average Nu is decreased with the increase of heated dimensionless length

References

[1] Mergui, S., Penot, F. "Natural convection in a differentially heated square cavity".Int. J. Heat mass Transfer, 1996.

[2] Taiy.S., Karayiayi, T.G, "Low turbulence natural convection in an air filled square cavity". Int. J. Heat mass transfer, 43,2000.

[3] M. Corcione, "Effects of thermal boundary condition at side walls upon natural convection in rectangular enclosure heated from below". Int. J. of thermal science ,vol.42,2003

[4] Ganzarolli, M. M. , "Natural convection in rectangular enclosures heated from below and symmetrically cooled from the sides". Int. J. Heat mass Transfer, 1995

[5] DOL, H. S., Hanjalic, K. "computational study of study of turbulent natural convection in a side heated-near-cubic enclosure at high Rayleigh number", Int. J. Heat mass Transfer, vol. 44,2001.

[6] Sarris, I. E. , Lekakis, N. S. Vlachos, "Natural convection in rectangular cavities heated locally from below", Int. J. Heat mass Transfer, vol.47, 2004.

[7] Raji A, Hasnaoui M, Zrikem Z. (1997),"Natural convection in Interacting cavities heated from below", Int. J. Numer. Method, 1997.

[8] Catton I, "Effect of wall conduction on the stability of a fluid in a rectangular region heated from below " , J. Heat transfer, 1972.

[9] Aydin, Wen-Jei-Yang, "Natural convection in enclosure with localized heating from below and symmetrical cooling from sides", Int. J. Numer.methods heat fluid flow 2000.

[10] Calcagni, B., Marsili,. F., Paroncini, M., "Natural convection heat transfer in square enclosures heated from below, Appl. Thermal Engrg. 2005.

[11] Launder, B. E., and Spalding, D. B., "The numerical computation of turbulent flows", comp. Methods Appl. Mech. Engng, 1974.

[12] S. V. Patankar and D. B. Spalding, " A calculation procedure for parabolic flow", Int. J. Heat Mass Transfer, 1972.

[13] Versteege, H. K., Malasekera, W., "An introduction of computational fluid dynamic", Hemisphere publishing corporation, United State of America, 1995

[14] Markatos, N. C. and Pericleous, K. A., "Laminar and turbulent natural convection in an enclosed cavity", Int. J. Heat Mass Transfer, vol. 27, 1984

Nomenclature

Symbol	Description	Units	Symbol	Description	Units
Cf	Friction coefficient	-	Greek symbols		
Cp	Isobaric specific heat of the fluid	J/kg K			
C_u,C1,C2	constants of the turbulent model	-	β	Isobaric cubical expansion coefficient of fluid	K^{-1}
G	Acceleration due to gravity,9.81	m/s^2	ε	dissipation rate of turbulent kinetic energy	m^2/s^3
H	Height of the enclosure	m	ψ	stream function	m^2/s
k	Thermal conductivity of fluid	W/m K	μ	dynamic viscosity	Ns/ m^2
K	Turbulent kinetic energy	m^2/s^2	μ_t	Turbulent viscosity	Ns/ m^2
L	Height of the heat portion on the side wall	m	υ	kinematic viscosity of fluid	m^2/s
Nu	Nusselt number	-	ρ	density of fluid	kg/m^3
Pr	Prandtl number	-	σ_k, σ_ε	effective Prandtl numbers	-
Q	Heat Flux	W/m^2	τ_w	wall shear stress	N/m^2
Ra	Rayleigh number	-	Subscripts		
St	Stanton number	-			
T	Temperature	K			
T_p	Temperature of near wall node	K	c	cold wall	
T_w	Temperature of wall	K	eff	Effective value	
u,v	horizontal and vertical velocity components	m/s	h	hot wall	
W	width of the enclosure	m	max	maximum value	
x,y	horizontal and vertical coordinate	m	t	Turbulent	

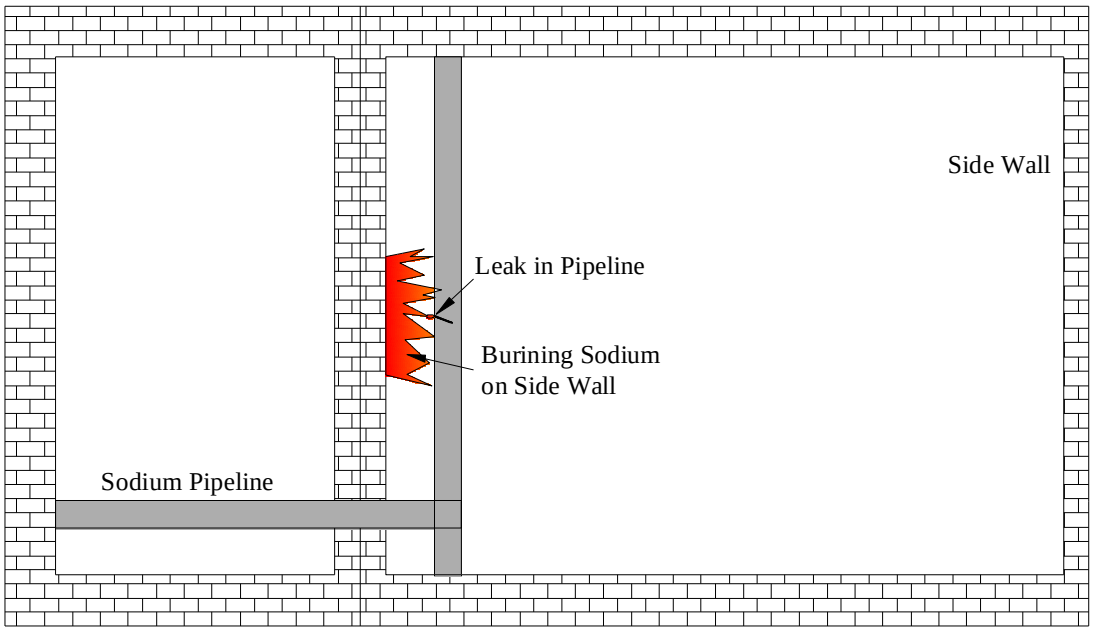

Figure (1) Schematic of the practical enclosure.

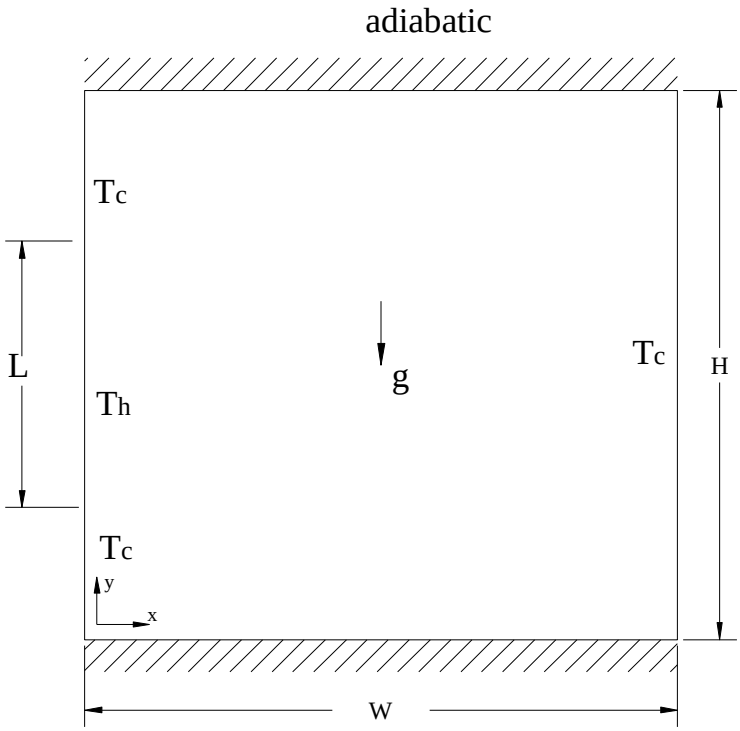

Figure(2) Physical model and boundary conditions.

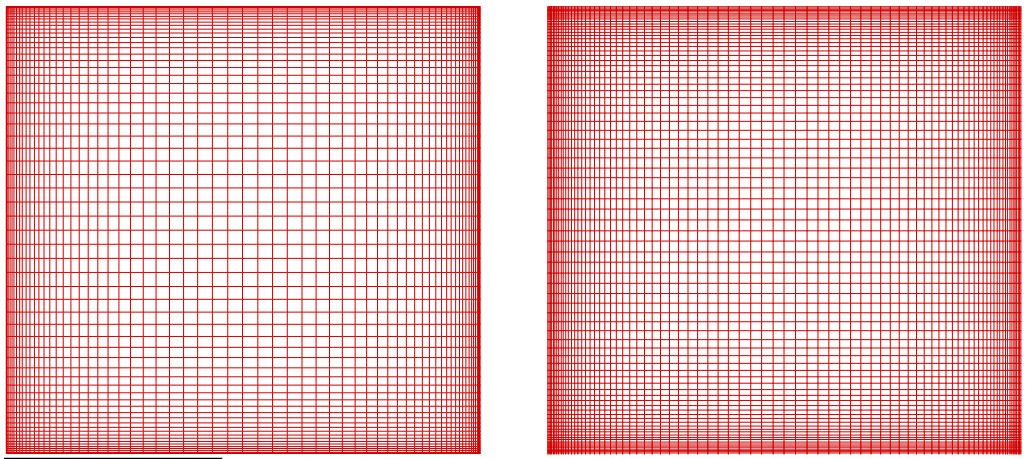

Figure (3) Grid pattern employed in the numerical computation.

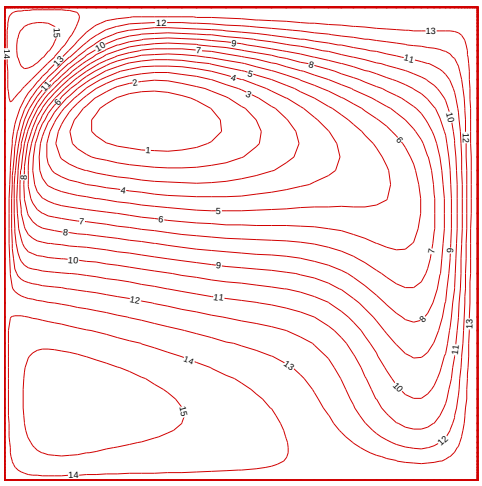

1

Level	Stream Line
15	2.49E-04
14	1.85E-05
13	-2.12E-04
12	-4.43E-04
11	-6.74E-04
10	-9.05E-04
9	-1.14E-03
8	-1.37E-03
7	-1.60E-03
6	-1.83E-03
5	-2.06E-03
4	-2.29E-03
3	-2.52E-03
2	-2.75E-03
1	-2.98E-03

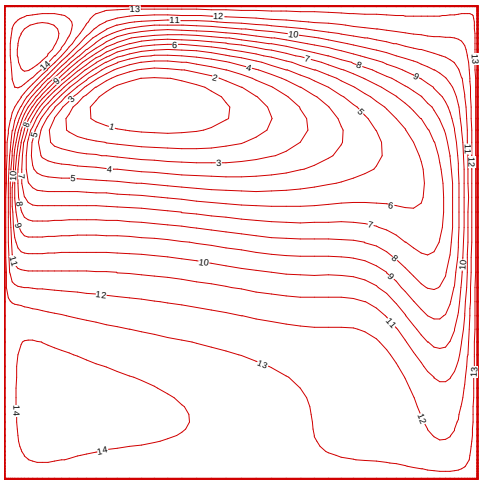

2

Level	Stream Line
15	1.06E-03
14	4.60E-04
13	-1.41E-04
12	-7.43E-04
11	-1.34E-03
10	-1.95E-03
9	-2.55E-03
8	-3.15E-03
7	-3.75E-03
6	-4.35E-03
5	-4.95E-03
4	-5.56E-03
3	-6.16E-03
2	-6.76E-03
1	-7.36E-03

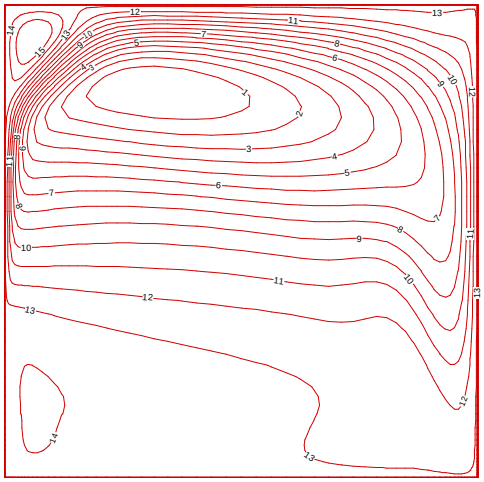

3

Level	Stream Line
15	3.37E-03
14	1.59E-03
13	-1.84E-04
12	-1.96E-03
11	-3.74E-03
10	-5.52E-03
9	-7.30E-03
8	-9.07E-03
7	-1.09E-02
6	-1.26E-02
5	-1.44E-02
4	-1.62E-02
3	-1.80E-02
2	-1.97E-02
1	-2.15E-02

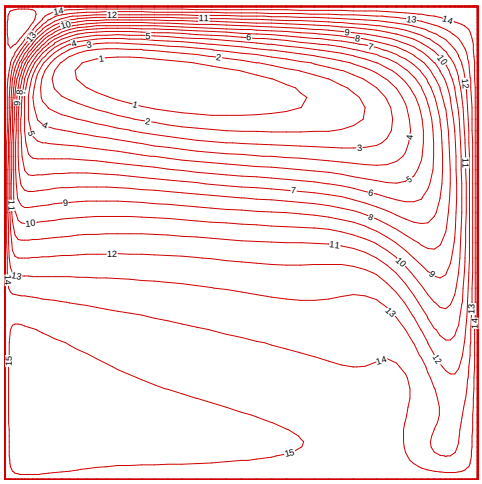

4

Level	Stream Line
15	1.61E-03
14	-3.76E-03
13	-9.13E-03
12	-1.45E-02
11	-1.99E-02
10	-2.52E-02
9	-3.06E-02
8	-3.60E-02
7	-4.14E-02
6	-4.67E-02
5	-5.21E-02
4	-5.75E-02
3	-6.28E-02
2	-6.82E-02
1	-7.36E-02

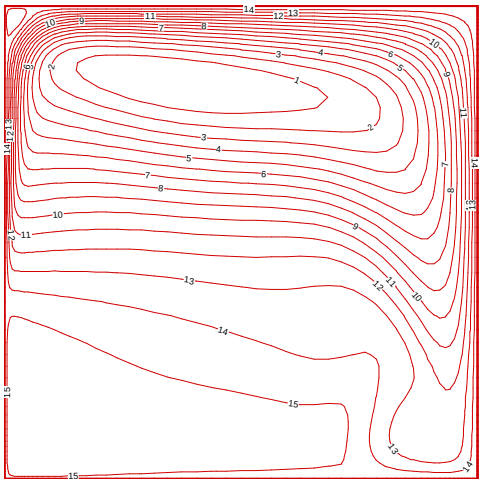

5

Level	Stream Line
15	2.81E-03
14	-1.40E-02
13	-3.09E-02
12	-4.77E-02
11	-6.45E-02
10	-8.14E-02
9	-9.82E-02
8	-1.15E-01
7	-1.32E-01
6	-1.49E-01
5	-1.66E-01
4	-1.82E-01
3	-1.99E-01
2	-2.16E-01
1	-2.33E-01

Figure4)Stream line (m^2/sec);L/H=0.2;(1)Ra=1E8: (2)Ra=1E9: (3)Ra=1E10: (4)Ra=1E11: (5)Ra=1E12

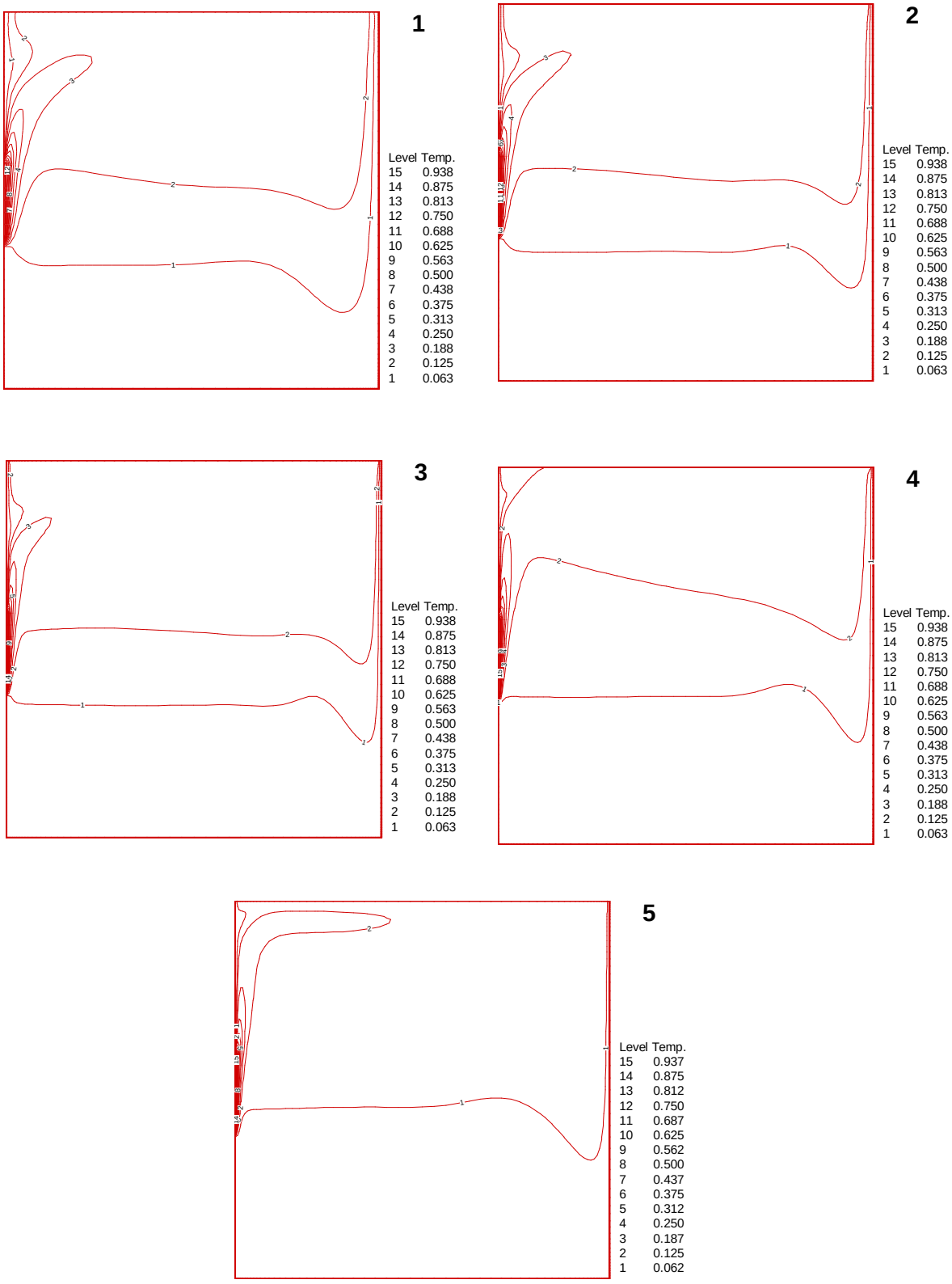

Fig.(5)Isotherms;$(T-T_c)/(T_h-T_c)$;L/H=0.2;(1)Ra=1E8: (2)Ra=1E9: (3)Ra=1E10: (4)Ra=1E11: (5)Ra=1E12

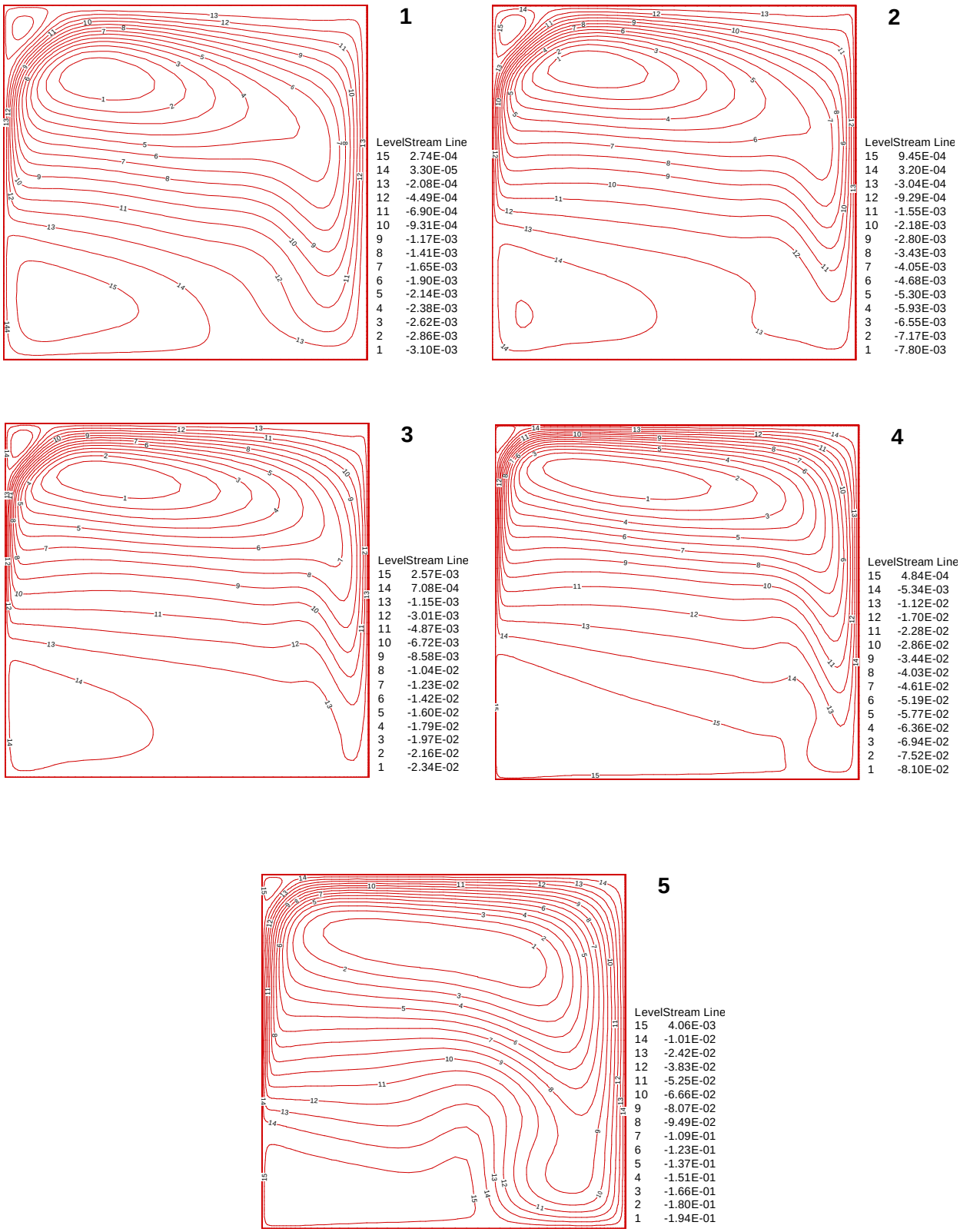

Fig.(6)Stream line (m^2/sec);L/H=0.4;(1)Ra=1E8: (2)Ra=1E9: (3)Ra=1E10: (4)Ra=1E11: (5)Ra=1E12

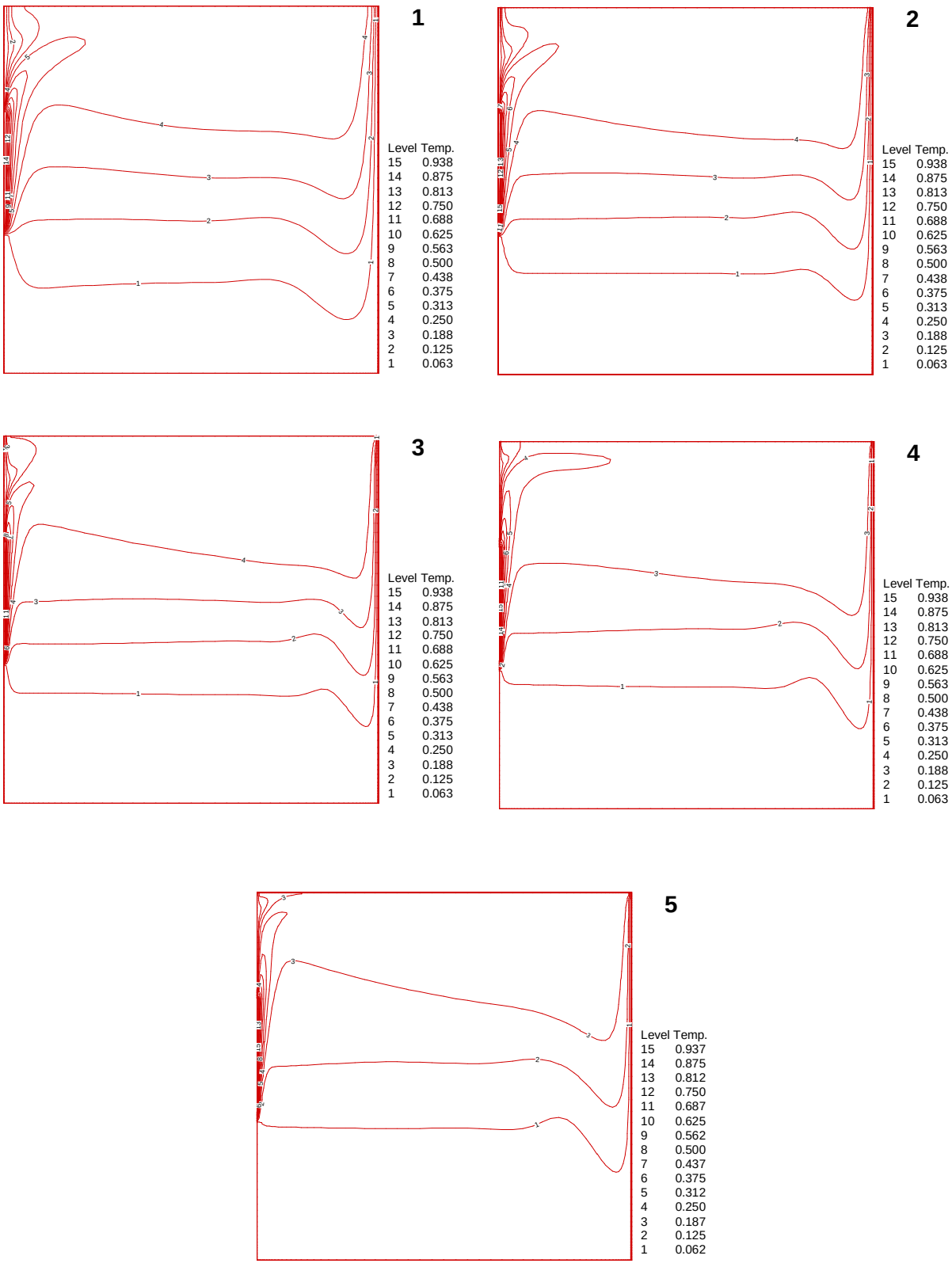

Fig.(7)Isotherms;$(T-T_c)/(T_h-T_c)$;L/H=0.4;(1)Ra=1E8: (2)Ra=1E9: (3)Ra=1E10: (4)Ra=1E11: (5)Ra=1E12

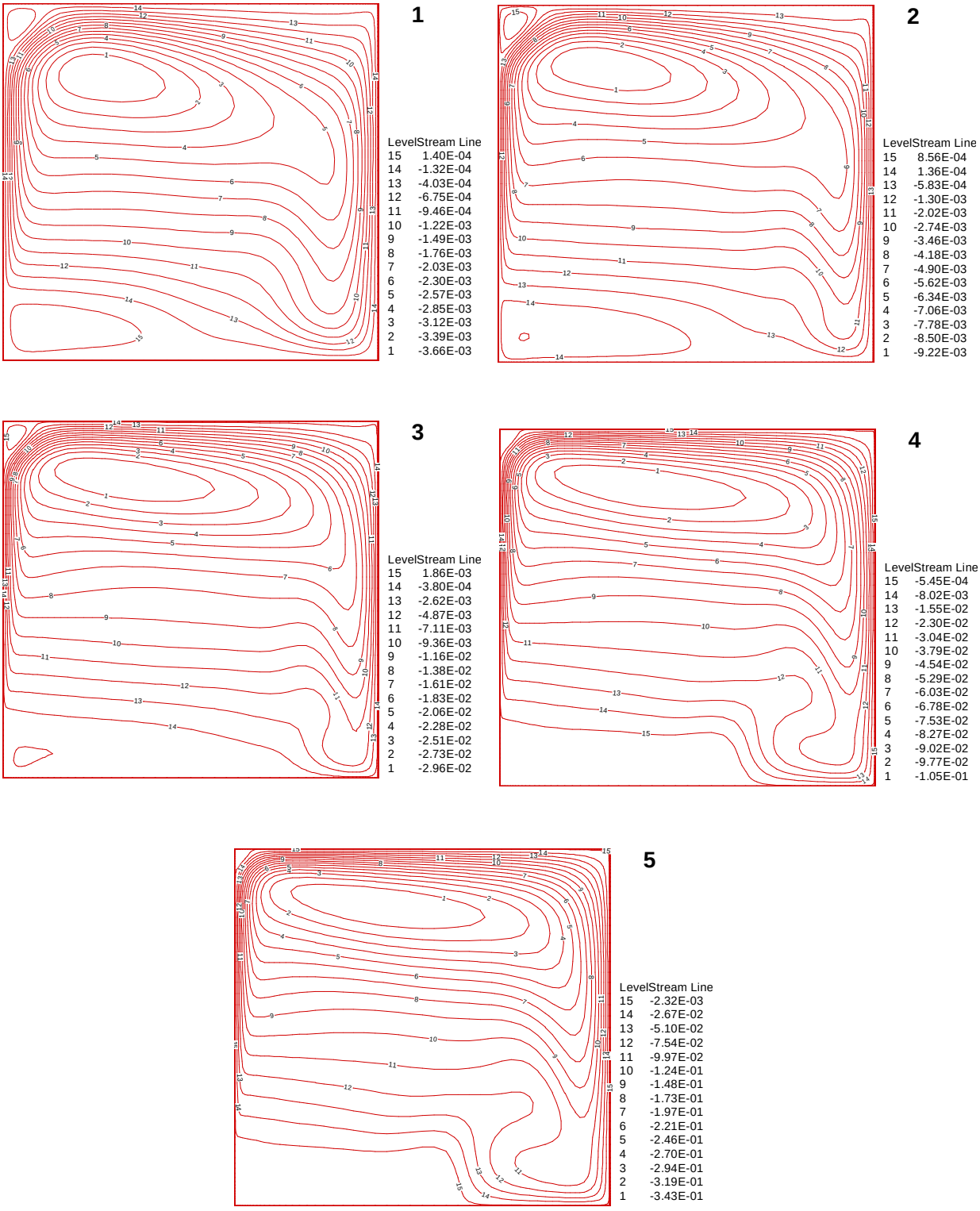

Fig.(8)Stream line (m^2/sec);L/H=0.6;(1)Ra=1E8: (2)Ra=1E9: (3)Ra=1E10: (4)Ra=1E11: (5)Ra=1E12

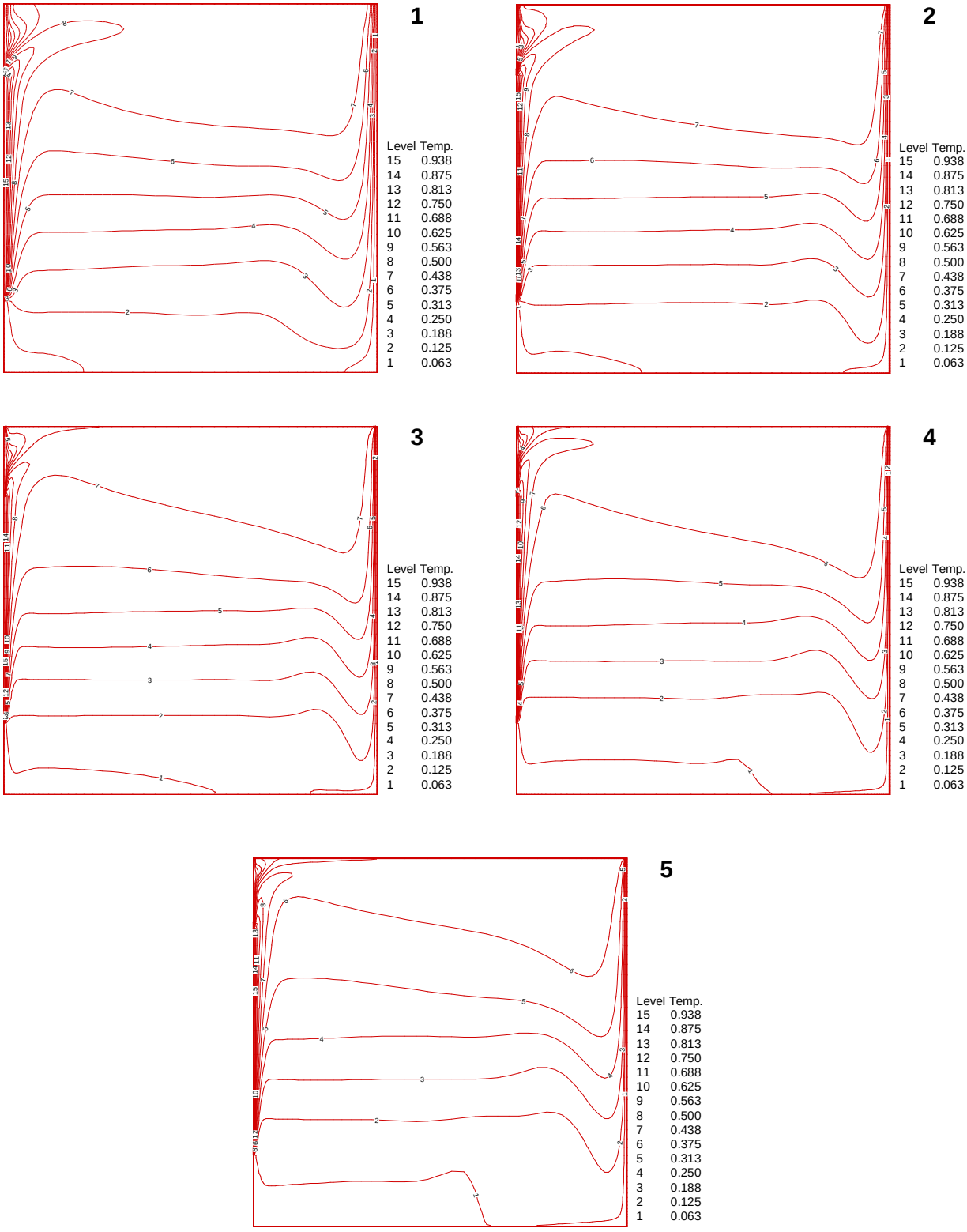

Fig.(9)Isotherms;$(T-T_c)/(T_h-T_c)$;L/H=0.6;(1)Ra=1E8: (2)Ra=1E9: (3)Ra=1E10: (4)Ra=1E11: (5)Ra=1E12

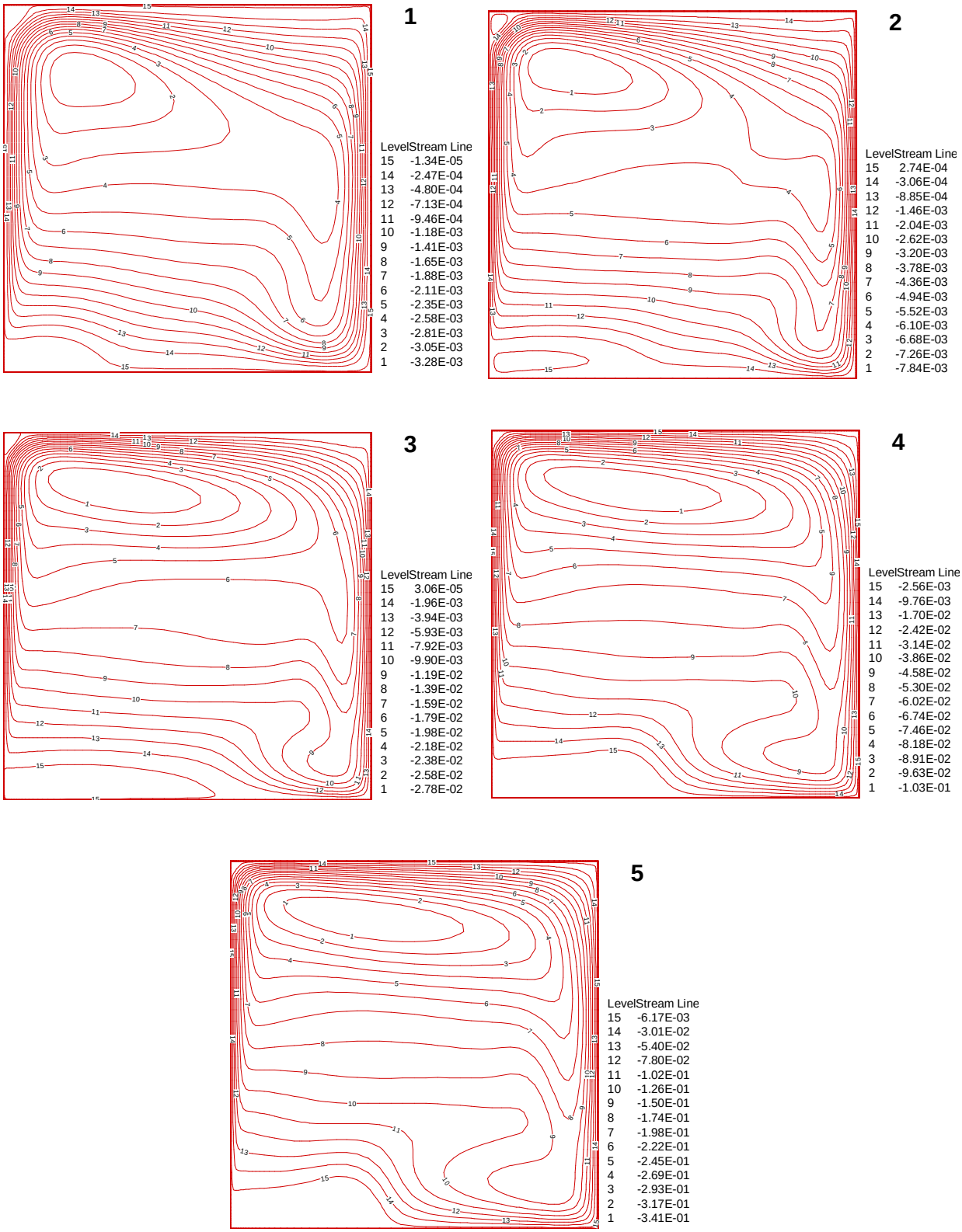

Fig.(10)Stream line (m^2/sec);L/H=0.8;(1)Ra=1E8: (2)Ra=1E9: (3)Ra=1E10: (4)Ra=1E11: (5)Ra=1E12

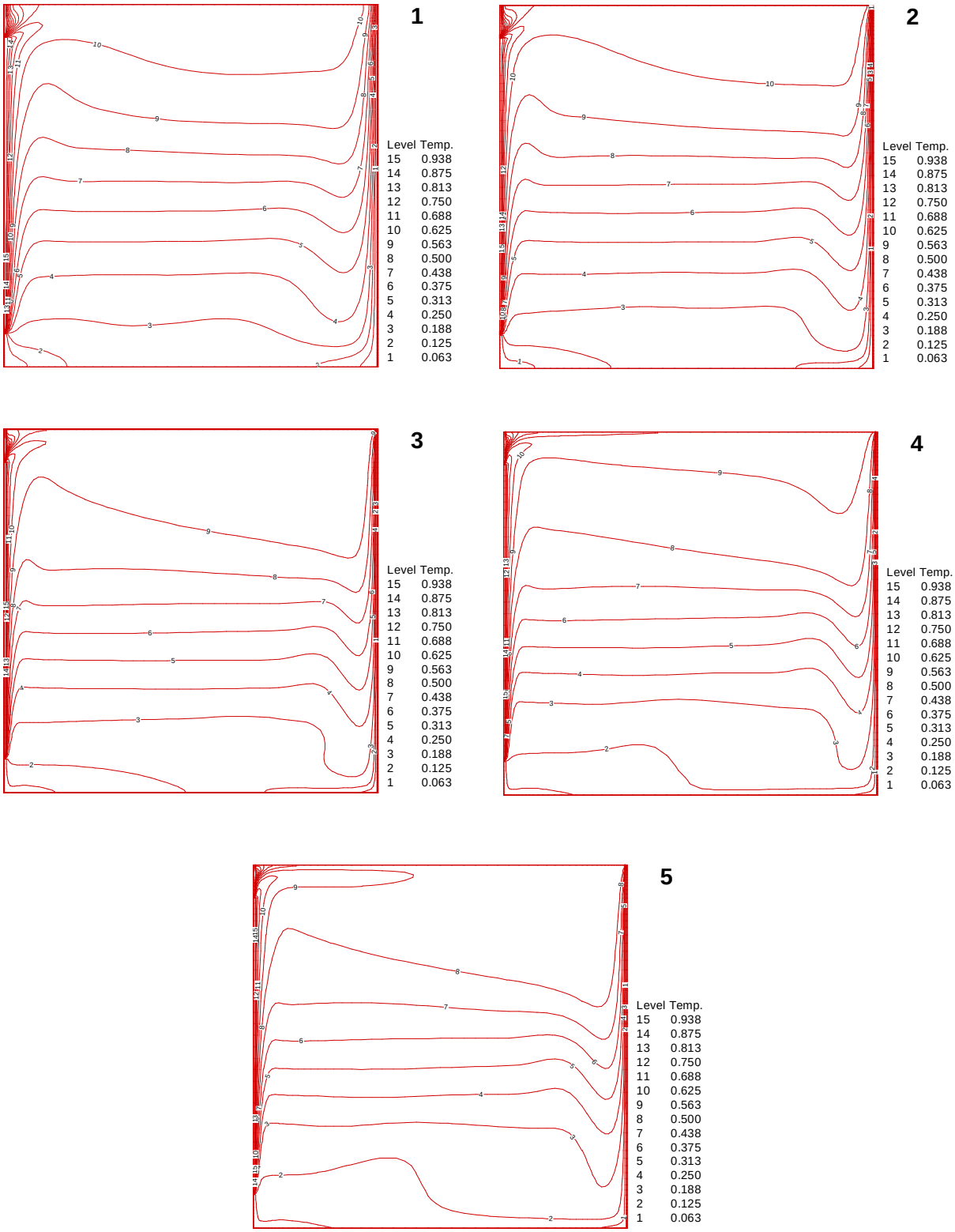

Fig.(11)Isotherms;$(T-T_c)/(T_h-T_c)$;L/H=0.8;(1)Ra=1E8: (2)Ra=1E9: (3)Ra=1E10: (4)Ra=1E11: (5)Ra=1E12

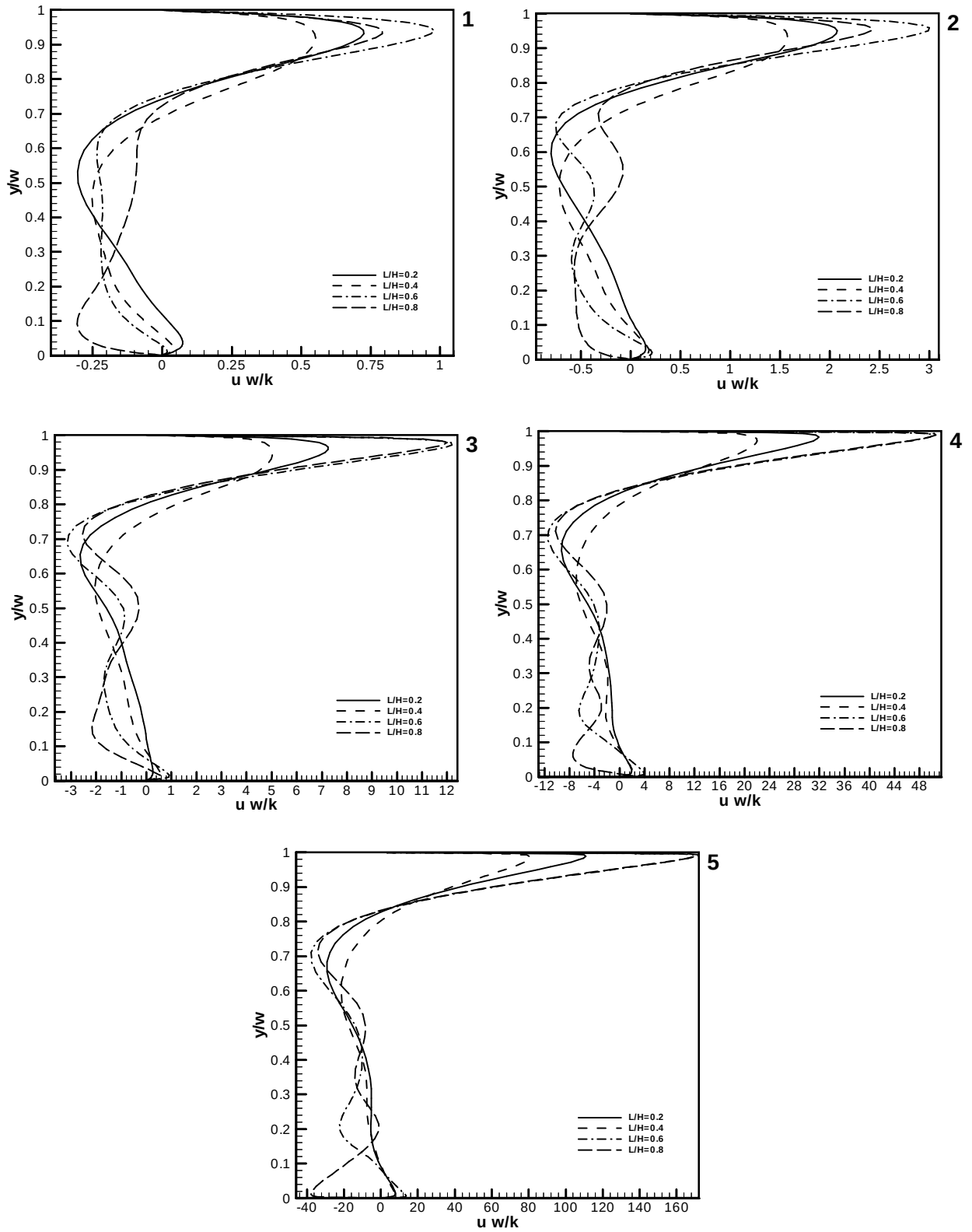

Fig.(12) The horizontal velocity component at x/W=1/2;(1)Ra=1E8: (2)Ra=1E9: (3)Ra=1E10: (4)Ra=1E11: (5)Ra=1E12

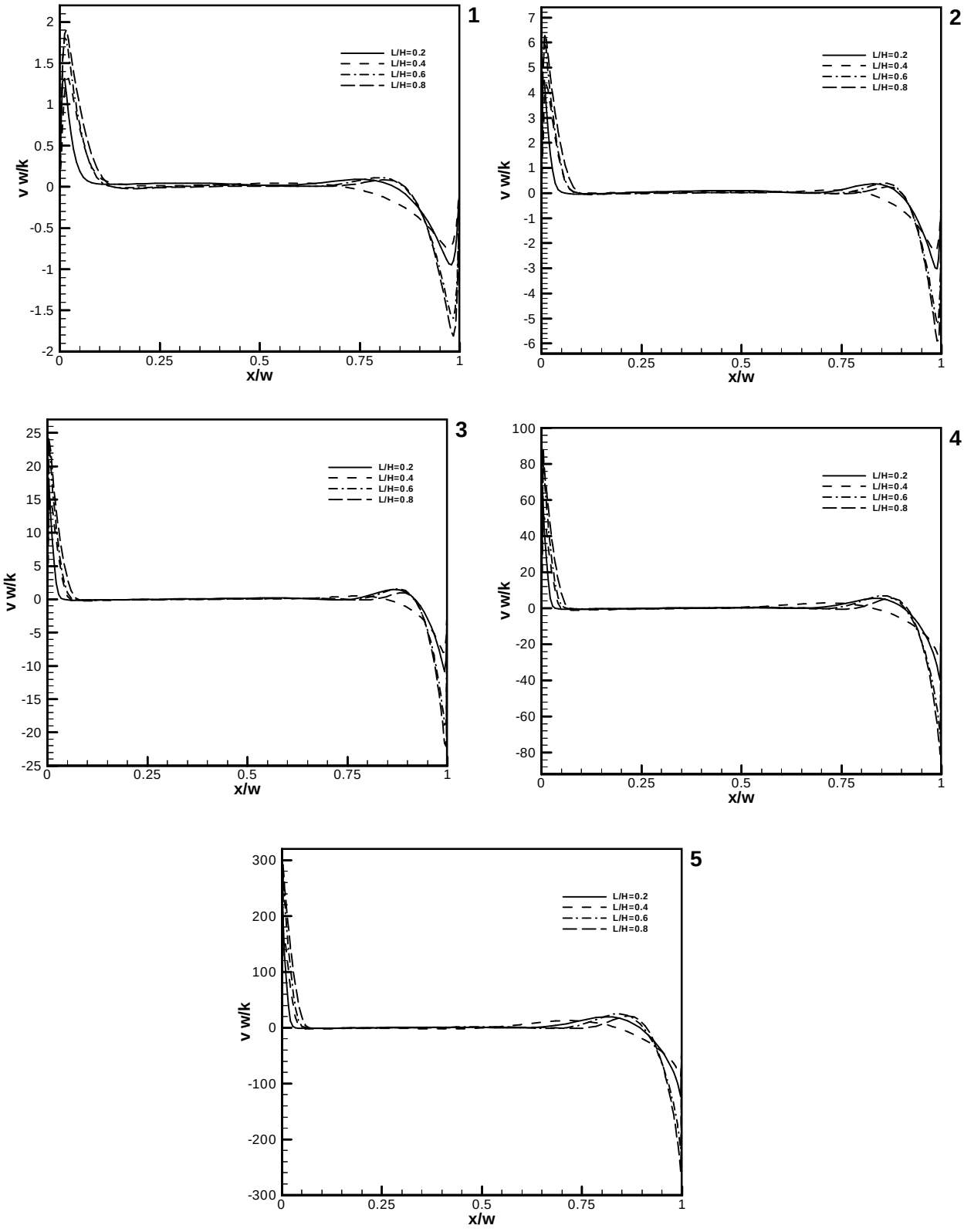

Fig.(13) The vertical velocity component at y/W=1/2;(1)Ra=1E8: (2)Ra=1E9: (3)Ra=1E10: (4)Ra=1E11: (5)Ra=1E12

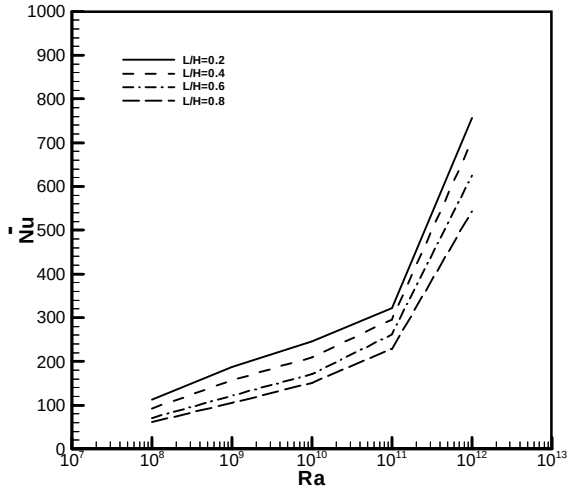

Fig.(14) Average Nusselt number versus Rayleigh number for dfferent L/H values.

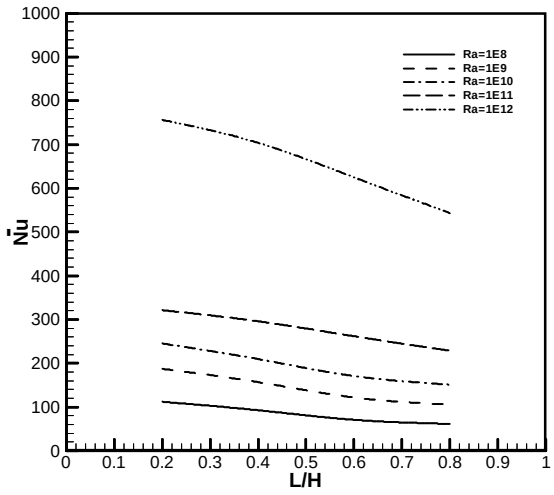

Fig.(15) Variation of average Nusselt number at heated wall versus L/H for diffrenet values of Ra.

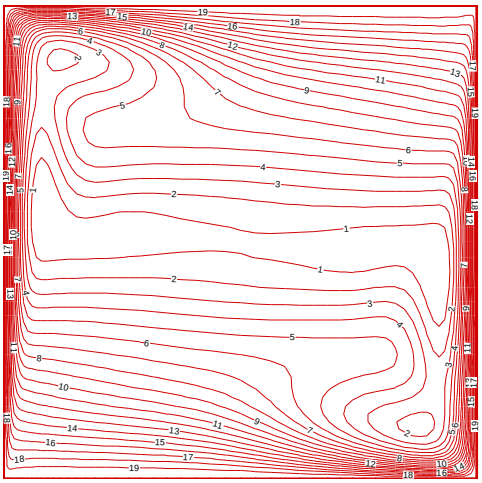

Level	Stream Lin
19	-9.13E-04
18	-1.84E-03
17	-2.77E-03
16	-3.69E-03
15	-4.62E-03
14	-5.55E-03
13	-6.47E-03
12	-7.40E-03
11	-8.32E-03
10	-9.25E-03
9	-1.02E-02
8	-1.11E-02
7	-1.20E-02
6	-1.30E-02
5	-1.39E-02
4	-1.48E-02
3	-1.57E-02
2	-1.67E-02
1	-1.76E-02

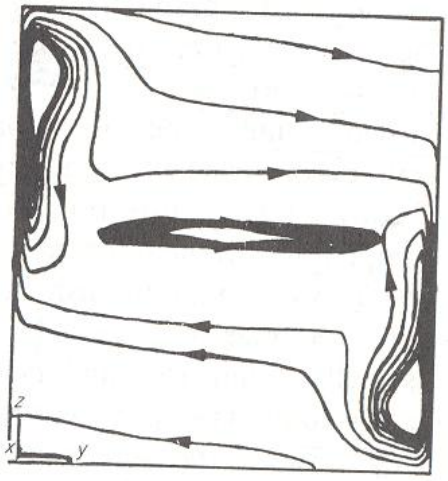

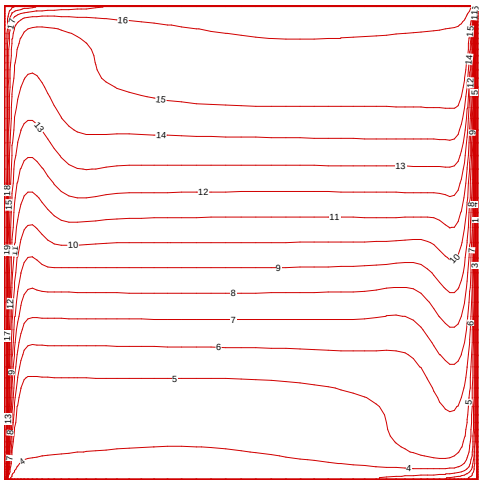

Level	Temp.
19	9.50E-01
18	9.00E-01
17	8.50E-01
16	8.00E-01
15	7.50E-01
14	7.00E-01
13	6.50E-01
12	6.00E-01
11	5.50E-01
10	5.00E-01
9	4.50E-01
8	4.00E-01
7	3.50E-01
6	3.00E-01
5	2.50E-01
4	2.00E-01
3	1.50E-01
2	1.00E-01
1	5.00E-02

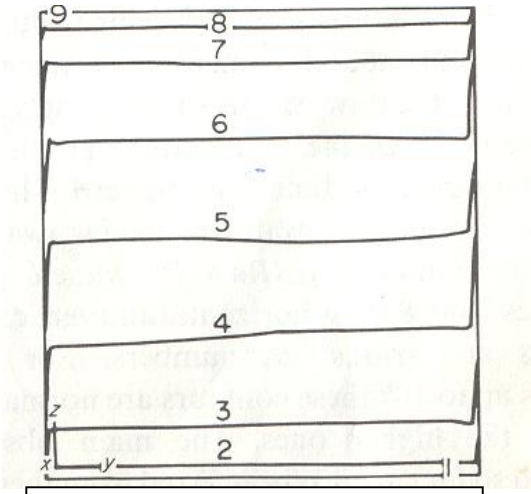

(a) present solution

(b) N. C. Markatos [14] solution

Fig.(16) Comparison of (a) present solution and (b)N. C. Markatos [14] solution at Ra=1E10 and L/H=1.0